

# General Applicability of Synthetic Gene-Overexpression for Cell-Type Ratio Control via Reprogramming

Kana Ishimatsu,<sup>†,‡,⊥</sup> Takashi Hata,<sup>†,⊥</sup> Atsushi Mochizuki,<sup>†,‡,§</sup> Ryoji Sekine,<sup>†</sup> Masayuki Yamamura,<sup>†</sup> and Daisuke Kiga<sup>\*,†,‡,||</sup>

<sup>†</sup>Department of Computational Intelligence and Systems Science, Tokyo Institute of Technology, Kanagawa 226-8503, Japan

<sup>‡</sup>PRESTO, Japan Science and Technology Agency, 7 Gobancho, Chiyodaku, Tokyo, 102-0076, Japan

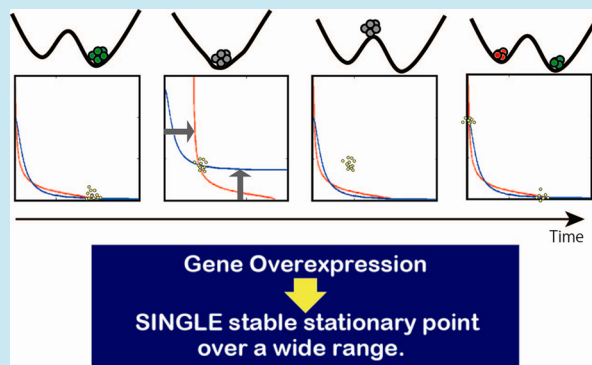
<sup>§</sup>Theoretical Biology Laboratory, RIKEN Advanced Science Institute, Wako, Saitama 351-0198, Japan

<sup>||</sup>Earth-Life Science Institute, Tokyo Institute of Technology, Meguro, Tokyo 152-8551, Japan

## S Supporting Information

**ABSTRACT:** Control of the cell-type ratio in multistable systems requires wide-range control of the initial states of cells. Here, using a synthetic circuit in *E. coli*, we describe the use of a simple gene-overexpression system combined with a bistable toggle switch, for the purposes of enabling the wide-range control of cellular states and thus generating arbitrary cell-type ratios. Theoretically, overexpression induction temporarily alters the bistable system to a monostable system, in which the location of the single steady state of cells can be manipulated over a wide range by regulating the overexpression levels. This induced cellular state becomes the initial state of the basal bistable system upon overexpression cessation, which restores the original bistable system. We experimentally demonstrated that the overexpression induced a monomodal cell distribution, and subsequent overexpression withdrawal generated a bimodal distribution. Furthermore, as designed theoretically, regulating the overexpression levels by adjusting the concentrations of small molecules generated arbitrary cell-type ratios.

**KEYWORDS:** cell-type ratio control, gene overexpression, multipotency



The control of a cell population capable of decision making to generate multiple cell-types is an important challenge for facilitating new frontiers in biology. The establishment of a generic strategy for population control is one of the goals of this endeavor and will be achieved through a fundamental understanding of multistability in genetic systems.<sup>1–3</sup> To acquire this understanding, synthetic biology bridges molecular biology and dynamics, by providing a platform to test dynamical systems.<sup>4–8</sup>

From the viewpoint of a dynamical system that can describe cellular decision-making and facilitate the development of a generic strategy for population control, the positions of the initial states of cells relative to the potential landscape of the multistable system determine the cell-type ratio of the population, as well as the type of each single cell. If the initial states of individual cells cross the watershed (i.e., separatrix) of the system (Figure 1A, left panel), then the final destinations of those cell states differ significantly (Figure 1A, right panel). As for the cell population, the distribution is divided into two subpopulations, when the initial cell states, exhibiting certain dispersion due to natural fluctuations, cross the separatrix (Figure 1B). Accordingly, controlling the initial states of cells is essential for the purpose of controlling cell-type ratios in the

multistable system. One limited strategy that can affect the initial cell states is to completely turn off the expression of the genes governing the multistable system,<sup>9</sup> thus placing the cell states at the origin point in the state space. However, this strategy is not generically applicable, since this method cannot destine the cell states for attractors with basins that do not include the point of origin.<sup>10–12</sup> Hence, a new strategy that can arbitrarily control the initial cell states over a much wider range is required.

Here, we utilized gene overexpression as the first generic strategy for the wide-range control of the initial cell states and thus for the arbitrary control of the ratios of cell types. Temporary gene-overexpression can place the cell states around a single site, by altering the system from a multistable to a monostable system (Figure 1C, the first panel to the second panel). The locations of these induced cell states can be controlled over a wide range, including sites far from the point of origin, by regulating the levels of overexpression. Upon cessation of the overexpression, this location of the induced cell states becomes the location of the initial states of the cells in

Received: August 2, 2013

Published: December 2, 2013

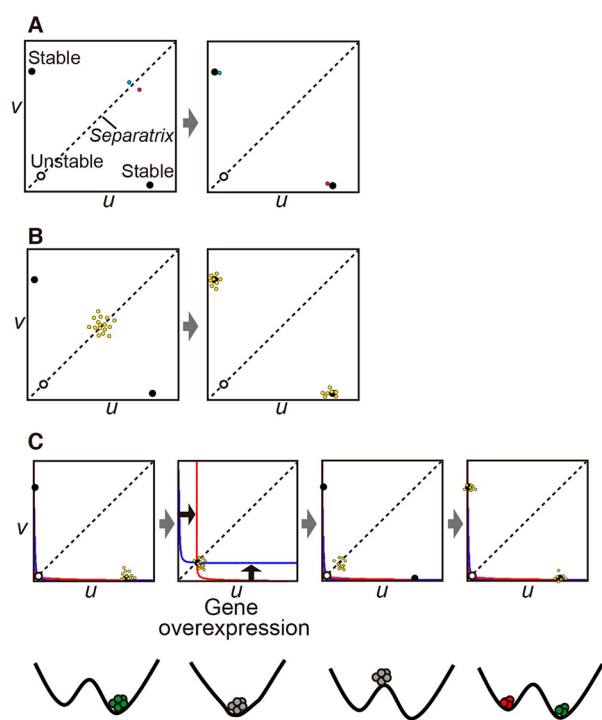


**Figure 1.** Modulation of a basal bistable system and cell-population control by gene overexpression. Each filled black circle represents a stable stationary point, and each open circle represents an unstable stationary point. Each cyan, magenta, and yellow dot represents the state of an individual cell. (A) The geometrical relationship between the initial state of a cell and the separatrix (left panel) determines the final state of the cell (right panel). The differently colored dots represent two cell states that initially have a small difference. When the initial cell states cross the separatrix, the difference between the cell states significantly increases. (B) A cell population initially crossing the separatrix becomes bimodal. (C) The overexpression of the toggle gene can control the nullcline and thus the final cell-type ratio. Regardless of the earlier states of the cells (the first panel is an example), the cell states are expected to converge to the single stable stationary point after the induction of toggle gene overexpression (second panel). The successive withdrawal of the overexpression (third panel) can redistribute the cell states (fourth panel). The lower panels show putative potential landscapes and the cell states on them, corresponding to the system statuses shown in the upper panels.

the basal multistable system (Figure 1C, the third panel). Setting the initial cell states on/around the separatrix of the basal system corresponds to cell-type reprogramming to a multipotent state, enabling the diversification of cells (Figure 1C, the fourth panel) with controlled cell-type ratios. In this study, as a proof-of-concept, we combined the synthetic overexpression circuit with the original toggle switch circuit (Figure 2),<sup>4</sup> which is the ideal model system for cell-type determination, and implemented the combined synthetic circuit within *E. coli*, as a model organism for generalized multicellular systems. We demonstrated that the fine and subtle manipulation of the initial cell states, through the regulation of gene-overexpression levels, indeed enabled the generation of arbitrary cell-type ratios. Furthermore, the mathematical analysis suggested that the overexpression strategy can be applied to various types of gene networks, owing to its ability to alleviate any nonlinearity of combined systems.

## RESULTS AND DISCUSSION

For the wide-range control of the initial cell states and the arbitrary control of the cell-type ratio, we designed a new system, named the controllable toggle, which is a combination of the original toggle switch subcircuit<sup>4</sup> and the overexpression subcircuit (Figure 2A). In this system, the overexpression level of each toggle gene is separately regulated, by adding the corresponding small molecules (Figure 2B). The number and the position of the stationary points of the controllable toggle can be understood by drawing the nullclines ( $du/dt = 0$ ,  $dv/dt = 0$  of eq 1) of the ordinary differential equations (ODEs) of this system. The ODEs can be described as follows:

$$\frac{du}{dt} = \frac{\alpha_1}{1 + v^\beta} - u + I_1 \quad (1)$$

$$\frac{dv}{dt} = \frac{\alpha_2}{1 + u^\gamma} - v + I_2$$

where  $u$  and  $v$  are the concentrations of the toggle regulators ( $u$  is the concentration of TetR and  $v$  is the concentration of LacI),  $\alpha_1$  and  $\alpha_2$  are the effective rates of synthesis of each regulator from the toggle subcircuit,  $\beta$  and  $\gamma$  are the cooperativities of the regulators, and  $I_1$  and  $I_2$  are the overexpression levels of each regulator.

Induction of overexpression in the controllable toggle model shifts the nullclines of the system, thus altering the number of stationary point(s) from 3 to 1. Parts A and B–D of Figure 3 illustrate the nullclines and stationary points of eqs 1 without and with overexpression, respectively (see also Figure 2B). Without overexpression ( $I_1 = I_2 = 0$ ), the nullclines intersect at three points under appropriate conditions: two are stable, and the other is an unstable stationary point (Figure 3A). For clarity, we call the system without the overexpression the ‘basal bistable system’. Meanwhile, with the overexpression of TetR ( $I_1 \gg 0$ ) and that of LacI ( $I_2 \gg 0$ ), each corresponding nullcline shifts toward the right and upward, respectively. Either or both of them cause a single intersection of the nullclines (Figure 3B–D), even though the parameters other than  $I_1$  and  $I_2$  are identical to those of the basal bistable system.

By varying  $I_1$  and  $I_2$ , wide-range control of a single stable stationary point is achieved in the state space (Figure 3E and F; Supporting Information Texts 1 and 2). The bifurcation set on the  $I_1 - I_2$  plane consists of two codimension-one open curves and a codimension-two point, at which the two codimension-one curves meet tangentially<sup>13</sup> (Figure 3E; Supporting Information Text 1). Importantly, in addition to the wide-range control of the single stable stationary point, fine and subtle control of the single stationary point can also be achieved, by independently regulating each overexpression level through adjustments of the corresponding small molecule concentration.

As shown in Figure 3G, the addition of the small molecules at appropriate concentrations and their subsequent removal are expected to change the nullclines and positions of the stable stationary points of the system, thus enabling the control of the cell population. Regardless of the previous distribution of the population (Figure 3G Step 1), appropriate overexpression makes the population converge to the single stationary point (Figures 2B and 3G Step 2). If the newly formed single stationary point is placed on/around the presumptive separatrix (Figure 3G Series C Step 2), then this step corresponds to the induction of a multipotent state. Upon overexpression withdrawal, which restores the system to the basal bistable

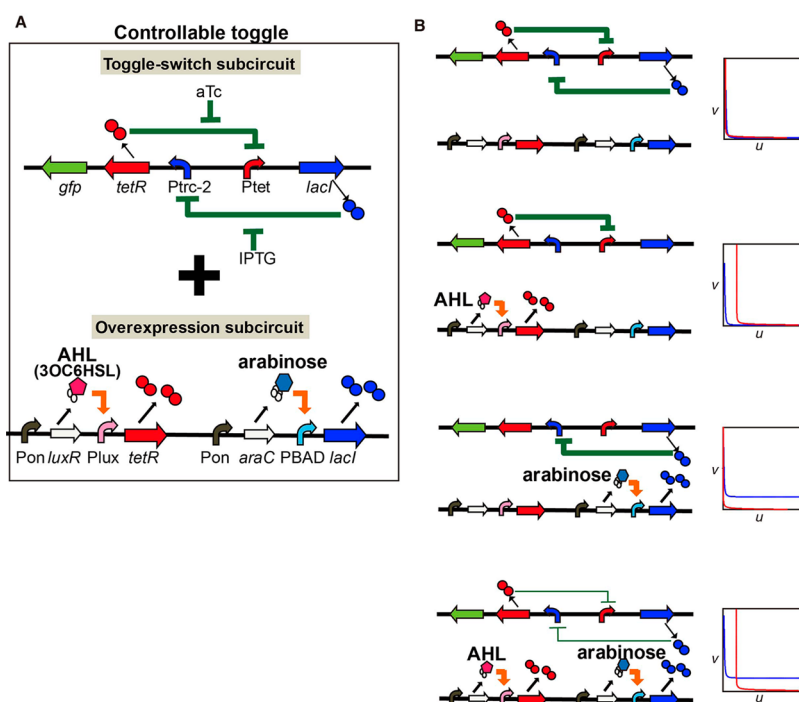


**Figure 2.** Design and function of a controllable toggle. (A) The controllable toggle consists of two subcircuits: a toggle switch and an overexpression subcircuit. The design of the toggle-switch subcircuit is almost the same as that in the original study.<sup>4</sup> In the overexpression subcircuit, TetR expression is induced by adding AHL, while LacI expression is induced by adding arabinose. (B) Effects of AHL and/or arabinose addition on the nullclines of the controllable toggle. The addition of each small molecule independently induces the overexpression of toggle genes (tetR and LacI), resulting in the shift in each nullcline.

system (Figure 3G Step 3), the location of the induced cell states (Figure 3G Step 2) becomes the location of the initial cell states in the basal system (Figure 3G Step 3). The cell population can then be redistributed (Figure 3G Step 4), depending on the geometric relationships between the initial cell states and the separatrix in Figure 3G Step 3. This system is expected to allow arbitrary control of the cell-type ratio, as shown in the heat map (Figure 3H) generated by a stochastic simulation<sup>14</sup> (Figure 3I).

The controllable toggle was implemented within living cells by introducing a set of two subcircuits (Figure 2A): one for the toggle switch, and the other for the overexpression of the two genes encoding the regulatory proteins of the toggle. The first subcircuit, the toggle switch, has almost the same design as that in the original study: *tetR* and *lacI* are arranged so that they inhibit each other's expression.<sup>4</sup> The *tetR* gene is under the control of *Ptrc-2*, which is negatively regulated by *LacI*, while *lacI* is controlled by *PLtetO-1*, which is negatively regulated by TetR. To monitor the dynamics of the controllable toggle, *gfpmut3* was placed so that it was simultaneously expressed with *tetR*. We define the 'high state' as the state where (GFP)*mut3* is highly expressed in the basal bistable system (Figure 3A). The opposite state, in which (GFP)*mut3* exhibits a low level of expression, is defined as the 'low state'. The second subcircuit, the overexpression subcircuit, contains four genes: *luxR*, *araC*, *tetR*, and *lacI*. The *luxR* and *araC* genes were placed under constitutive promoters (*Pon*). The *tetR* gene was placed under the promoter (*Plux*), which is positively regulated by LuxR in the presence of acyl-homoserine lactone (AHL). Meanwhile, the *lacI* gene was controlled by the promoter (*PBAD*), which is positively regulated by AraC in the presence of arabinose. The overexpression subcircuit was designed so that the expression levels of *tetR* and *lacI* could be

independently regulated by adjusting the amounts of AHL and arabinose, respectively. The two subcircuits were introduced into the *E. coli* strain JM2.300 for the following experiments.

To confirm the ability of our controllable toggle to control the locations of the initial cell states, which determine the cell-type ratio of the final population, we first evaluated the effects of the overexpression of each regulatory protein, by adding the corresponding molecule (corresponding to Figure 3G Series A and B). Before induction to the initial state by gene overexpression, the controllable toggle cells were set near the low state by adding anhydrotetracycline hydrochloride (aTc), which inhibits TetR activity (Figure 4A). After the system was restored to the basal bistable system by removing aTc (Figure 4B), AHL was added to the medium for the overexpression of TetR, to induce the cells to the initial state. As a result, the cell states switched from the low state to near the high state (Figure 4C). In addition, after the removal of AHL, the cell population remained in the high state for at least 10 h (Figure 4D). The opposite result (Figure 4E–H) was obtained when the corresponding experiment was started from the cells set to the high state, by adding and successively removing isopropyl- $\beta$ -D-thiogalactopyranoside (IPTG) (Figure 4E and F). The cell states were switched from the high state to near the low state by adding arabinose (Figure 4G) and remained in the low state after the arabinose was removed (Figure 4H). In addition, when the induction did not switch the cell state, the cell states remained in the high or low state after the removal of AHL or arabinose (Figure 4I–P). These results were consistent with the expected situations represented in Figure 3G Series A and B, confirming that the overexpression of each gene in the controllable toggle can shift the nullclines and control the locations of the initial cell states.

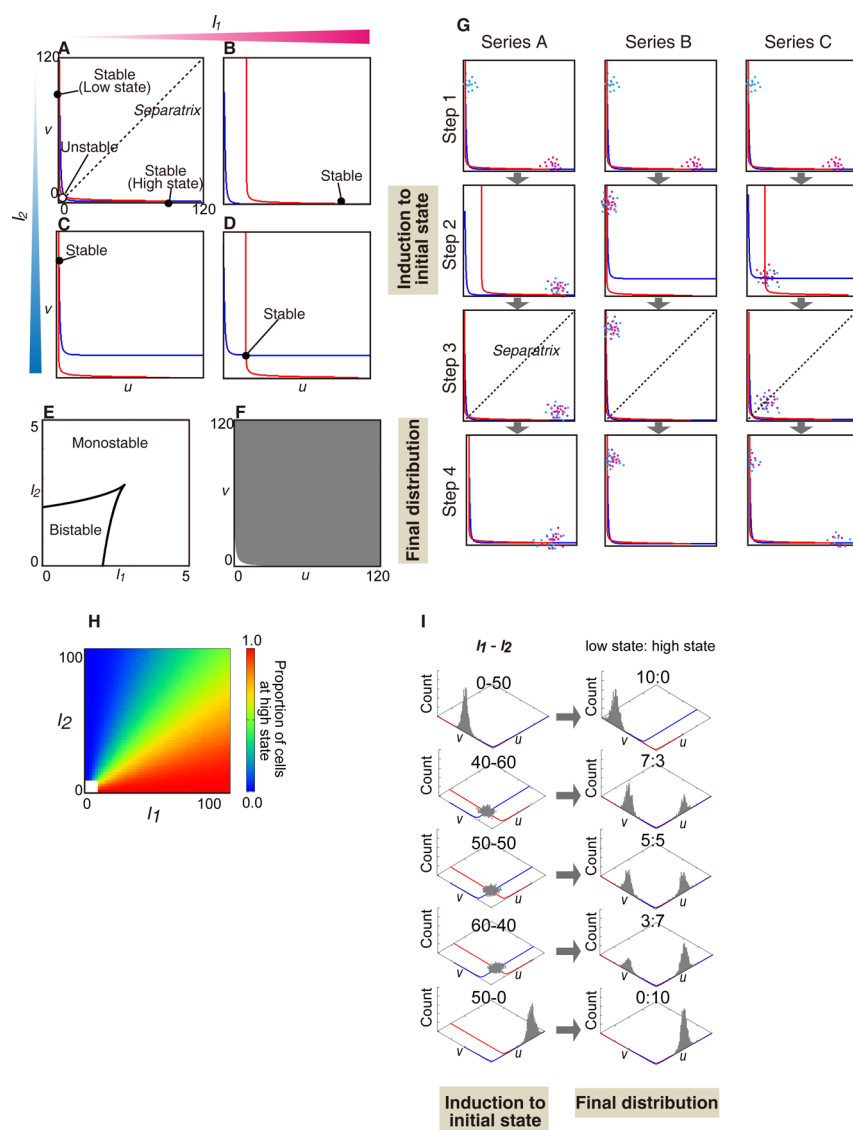


**Figure 3.** Theoretical expectations for the controllable toggle system. The red curves correspond to the nullcline  $du/dt = 0$ , and the blue curves correspond to the nullcline  $dv/dt = 0$ . Nullclines and stationary points without (A) and with (B–D) overexpression. (E) Bifurcation set in the  $I_1 - I_2$  plane. (F) The colored region is the area over which the controllable toggle can generate the single stable stationary point. (G) Expected changes in nullclines and cell distributions in overexpression experiments. Series A, B, and C only differ in the amounts of the overexpressed gene product(s); LacI, TetR, and both are induced in series A, B, and C, respectively. Cyan and magenta dots respectively represent cell states that are set to the low and high states in Step 1. States before overexpression is induced (Step 1), while the overexpression is induced (Step 2), immediately after the overexpression is withdrawn (Step 3), and a certain time after the overexpression is withdrawn (Step 4) are represented in a time course. (H, I) Relationship between the  $I_1 - I_2$  values upon overexpression induction and the cell-type ratio of the final state distribution, calculated by stochastic simulation and demonstrated by the heat map (H) and the histogram (I). (H) Using various values of  $I_1 - I_2$ , each ranging from 0 to 100, the cell-type ratios of the final distribution corresponding to each  $I_1 - I_2$  value set are mapped. (I) Demonstration of numerical experiments performed by stochastic simulation. The  $I_1 - I_2$  values at the initial states and the cell-type ratio in the final distribution are indicated in each panel.

We next examined whether we could actually create bimodal distributions, via an induced monomodal initial state, by simultaneously inducing the overexpression of both regulator proteins (corresponding to Figure 3G Series C). After the cells were set to either the high or low state by adding (Figure 5A and B) and subsequently removing IPTG or aTc (Figure 5C and D), adding both AHL and arabinose induced both samples to identical initial states (Figure 5E and F). In contrast to the addition of either AHL or arabinose (Figure 4), the population was located between the high and low states in this experiment. At 10 h after the removal of AHL and arabinose, the monomodal distribution spread and became a completely bimodal distribution in the restored basal bistable system

(Figure 5G and H). These results were consistent with our expectation that a cell population initially located in an appropriate range, between the high and low states, would exhibit a bimodal distribution in the successive basal bistable system (Figure 3G Series C). Furthermore, we finely controlled the cell-type ratio of the final population, by tuning the locations of the initial population through modulations of the overexpression levels (Figure 5I), as intended by dynamical system-based design (Figure 3G–I). The controllable toggle cells were induced with one of the nine combinations of AHL and arabinose concentrations. Ten hours after the removal of AHL and arabinose, the subtle variations in the AHL and arabinose concentrations resulted in differences in the ratios of

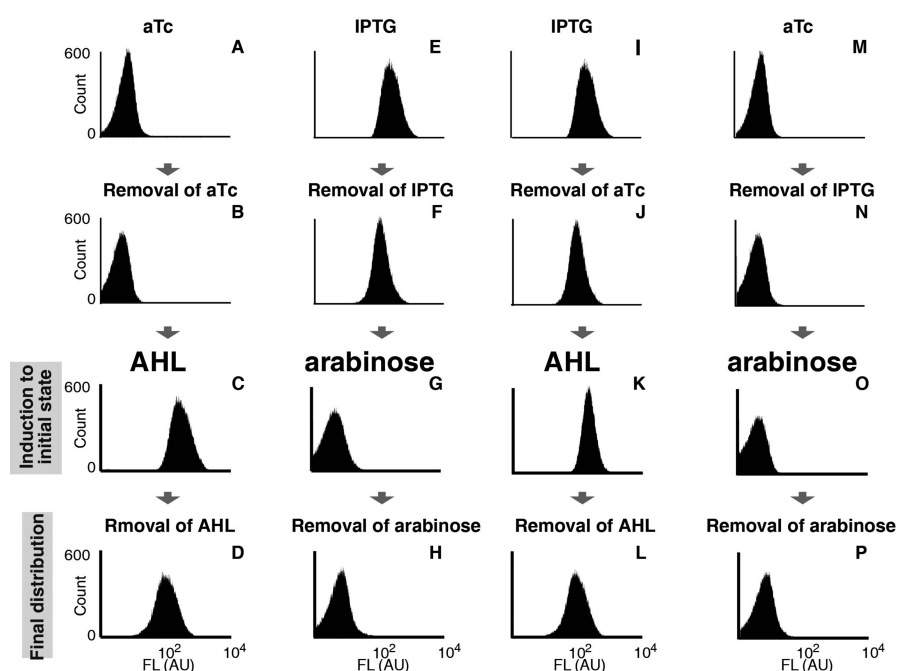


**Figure 4.** Effects of the overexpression of one gene. (A, E, I, M) Before being induced to the initial state, the cells are set to near the high or low state by IPTG or aTc, respectively. (B, F, J, N) IPTG or aTc is then removed from the growth media. (C, G, K, O) The overexpression of TetR or LacI is induced by adding AHL or arabinose, respectively, thus setting the cells to the initial states. (D, H, L, P) The positions of the cell states remain almost the same, from the initial distribution to the final distribution, 10 h after the removal of AHL or arabinose.

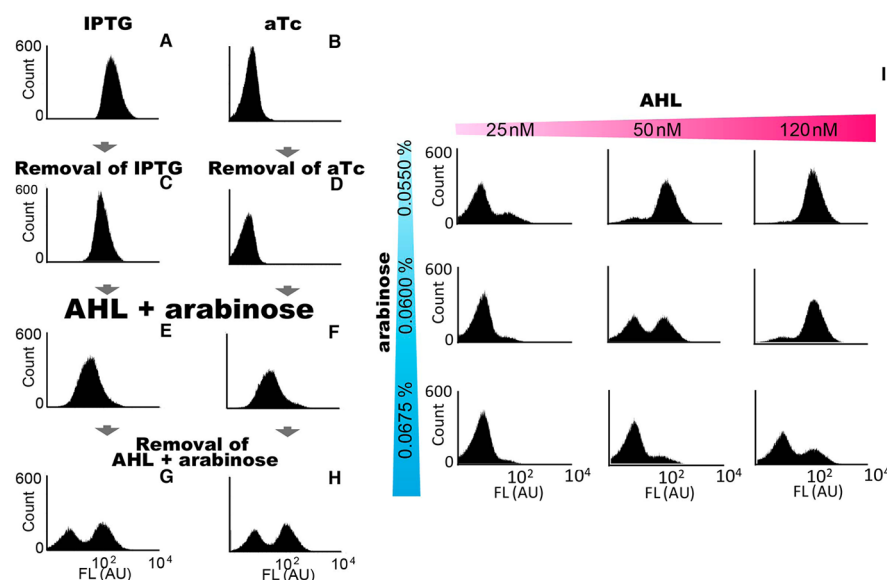


**Figure 5.** Effects of the overexpression of both genes. (A, B) Before being induced to the initial state, the cells are set to near the high or low state by IPTG or aTc, respectively. (C, D) IPTG or aTc is then removed from the growth media. (E, F) The overexpression of both TetR and LacI is induced by adding both AHL and arabinose. (G, H) The cells exhibit the final bimodal distribution 10 h after the removal of AHL and arabinose. (I) Final distributions under different induction conditions. The cells were initially induced with one of the nine combinations of AHL and arabinose concentrations, as indicated in the figure. Subtle differences in the concentrations change the final distributions of the cells.

the high to low state cells (Figure 5I). These results indicated that tuning the overexpression levels indeed changes the geometric relationship between the initial cell states and the separatrix.

Our synthetic gene network provides the first generic strategy for controlling the initial cell states over a wide range, and for arbitrarily controlling the cell-type ratio in a multistable system. In multistable systems, the initial states of the cells, as well as the landscape itself of the system, are

theoretically considered to be essential in determining the dynamics of cells, especially when the initial states are located on/around the separatrix. However, despite the importance of the initial states, their arbitrary manipulation had not been attempted. Although a previous study<sup>9</sup> showed that the initial cell states can be set at the point of origin by completely shutting off the genes governing the bistability, this strategy is not suitable for placing the initial state at other sites. Our overexpression strategy is the first direct demonstration of the

effects of the initial cell states, controlled over a wide range, on the cellular dynamics.

While we have established the control strategy for two-gene systems of mutual inhibition in living cells, this generic manipulation strategy can be generalized to an  $N$ -dimensional ODE system characterized by the following equation:

$$\frac{dx_i}{dt} = f_i(x_1, \dots, x_n) - x_i + I_i \quad i = 1, \dots, N \quad (2)$$

in which  $f_i$  is a positive nonlinear function and  $I_i$  is a constant for overexpression. When we increase  $I_i$  relative to  $f_i$  ( $I_i \gg f_i$ ) for each  $i$ , the nullcline shifts toward the positive direction of each  $i$ -axis, and is close to the hyperplane  $x_i = I_i$ . At this point, the system becomes “positive constant production with linear decay” and produces a single stable stationary point  $I = (I_1, \dots, I_n)$ . Note that this argument does not depend on the reaction term  $f_i$ . Although this strategy requires high levels of expression, it offers a substantial advantage for controlling living cells, which are governed by prominent nonlinearities. In contrast, significant technical difficulties generally exist when attempting to directly change the nonlinearity, such as the Hill coefficient of each biochemical reaction.<sup>15</sup> This feature of the overexpression strategy offers broad applicability in various types of gene networks (an example of a more complex network is shown in Supporting Information Figure 1)

The cell-type ratio is an important issue in many biological systems and engineering applications. It is required for various multicellular organisms, ranging from simple social amoeba<sup>16</sup> to vertebrates,<sup>17–19</sup> to ensure that their bodies and tissues consist of the appropriate ratios of constituent cells to perform their functional roles. In addition, from the view of potential applications, the biosynthesis of medically and industrially important compounds using microbial consortia can achieve optimal efficiency when the consortia are composed of several types of cells with a specific cell-type ratio.<sup>20</sup> Since our controllable toggle enables the arbitrary control of the cell-type ratio, it will play significant roles for understanding natural systems and developing medical and industrial applications in relation to the cell-type ratios.

## METHODS

**Enzymes, Chemicals, and Strain.** Restriction enzymes and polynucleotide kinase were purchased from New England Biolabs, TOYOBO, and TaKaRa. All oligonucleotides were from Operon Technologies, Inc. Isopropyl- $\beta$ -D-thiogalactopyranoside (IPTG) and standard chemicals were purchased from Nacalai, L-(+)-arabinose was from Wako, anhydrotetracycline hydrochloride (aTc) was from Rieden-de Haen, and N-( $\beta$ -ketocaproyl)-DL-homoserine lactone was from Sigma-Aldrich Japan. Polymerase chain reaction (PCR) was performed with KOD-Plus polymerase (TOYOBO). The host cell line for all experiments was *E. coli* strain JM2.300 (l-, lacI22 rpsL135 (StrR), thi-1).<sup>7</sup>

**Plasmid Construction.** The plasmids used in this work are shown in Supporting Information Figure 2. pETS101 (LacI TetR toggle) was kindly provided by J. J. Collins. The overexpression subcircuit was basically constructed by combining Pon-*luxR* (altered from Ptet-*luxR*<sup>7</sup>), Plux-*tetR* (altered from pETS101) and Pon-*lacI*-Pbad-*araC* (BioBrick K395402). Details are described in the Supporting Information Methods.

**Assay Protocol.** In all of the following steps, the cells were incubated at 37 °C. An overnight culture of cells harboring both pETS101 and an overexpression plasmid was diluted 1:2000

into 3.0 mL of fresh “basal medium”, LB medium with antibiotics (50  $\mu$ g/mL carbenicillin and 30  $\mu$ g/mL kanamycin), and then grown until the cell population reached a sufficient density ( $OD_{590} = 0.35 \pm 0.05$ ). The cells were then diluted into 3.0 mL of medium containing either 0.1 mM IPTG or 5  $\mu$ g/mL aTc, and grown for 2 h until the cell population reached a sufficient density ( $OD_{590} = 0.35 \pm 0.05$ ) (Figures 4A, E, I, M and 5A, B). A 1.0 mL aliquot of the culture was washed with 1.0 mL of fresh basal medium by centrifugation, and subsequently incubated in 3 mL of basal medium for 3 h (Figures 4B, F, J, N and 5C, D). To induce the initial cell states (Figures 4C, G, K, O and 5E, F), the cells were diluted 1:3500 in 3 mL of medium containing AHL and/or arabinose (concentrations indicated in the figures), and were incubated for 6 h. To restore the basal bistable system (Figure 4D, H, L, P and 5G, H, I), 1.0 mL of the culture was washed with 1.0 mL of fresh basal medium by centrifugation. The washed cells were then incubated in 3 mL of basal medium for 10 h, with dilution in fresh basal medium every 2 h. Samples were removed for flow cytometry analyses over the course of the experiment.

**Fluorescence Measurements.** All fluorescence data were collected using a Becton-Dickinson FACSCalibur flow cytometer, with a 488-nm laser and a 515–545-nm emission filter. Before measurement, the cells were washed with PBS by centrifugation.

**Numerics.** All of the nullclines were calculated numerically with eq 1 ( $\alpha_1 = \alpha_2 = 100$ ,  $\beta = \gamma = 2$ ), using the Matlab (Mathworks) and Maxima programs (available at <http://maxima.sourceforge.net/>). Stochastic simulations were performed according to the procedures reported by Sekine et al.<sup>7</sup>

**Determination of the Region of the Single Stable Stationary Point Achieved by Gene Overexpression.** In summary, the bifurcation set on the  $I_1 - I_2$  plane (Figure 3E) was determined from the conditions in which the nullclines of eq 1 have a point of tangency. In Figure 3F, the boundary of the region of the single stable steady point was calculated using the pairs of ( $I_1, I_2$ ) coordinate values on the bifurcation set. Details are described in the Supporting Information Texts 1 and 2.

## ASSOCIATED CONTENT

### Supporting Information

Additional methods, text, and figures as described. This material is available free of charge *via* the Internet at <http://pubs.acs.org>.

## AUTHOR INFORMATION

### Corresponding Author

\*Tel./Fax: +81-45-924-5213. E-mail: [kiga@dis.titech.ac.jp](mailto:kiga@dis.titech.ac.jp).

### Author Contributions

<sup>†</sup>K.I. and T.H. contributed equally to this work. K.I. and D.K. conceived the study. K.I., T.H., and D.K. designed the experiments. K.I. and T.H. performed the experiments. All of the authors took part in the interpretation of the results and the preparation of the manuscript.

### Notes

The authors declare no competing financial interest.

## ACKNOWLEDGMENTS

We thank J. J. Collins (Boston University) for providing pETS101 (LacI TetR toggle) and Y. Kabashima (Tokyo Tech.), K. Aihara (University of Tokyo), K. Nishimura (University of Tsukuba), S. Kitano (Tokyo Tech.), and all of our PRESTO colleagues for crucial discussions. We also thank A. Kaneko

(Professor Emeritus, University of Tokyo and Ochanomizu University) for numerical analysis instruction. This work was supported by the JST PRESTO program (D.K.) and the MEXT KAKENHI programs (23119005 to D.K.) and JSPS (23680031 to D.K.), and in part by an HFSP program grant (A.M.). K.I. was partially supported by Research Fellowships for Young Scientists from JSPS.

## ■ REFERENCES

- (1) Balazsi, G., van Oudenaarden, A., and Collins, J. J. (2011) Cellular decision making and biological noise: From microbes to mammals. *Cell* 144, 910–25.
- (2) Ferrell, J. E., Jr. (2012) Bistability, bifurcations, and Waddington's epigenetic landscape. *Curr. Biol.* 22, R458–66.
- (3) Furusawa, C., and Kaneko, K. (2012) A dynamical-systems view of stem cell biology. *Science* 338, 215–7.
- (4) Gardner, T. S., Cantor, C. R., and Collins, J. J. (2000) Construction of a genetic toggle switch in *Escherichia coli*. *Nature* 403, 339–42.
- (5) Kramer, B. P., Viretta, A. U., Daoud-El-Baba, M., Aubel, D., Weber, W., and Fussenegger, M. (2004) An engineered epigenetic transgene switch in mammalian cells. *Nat. Biotechnol.* 22, 867–70.
- (6) Lim, W. A., Lee, C. M., and Tang, C. (2013) Design principles of regulatory networks: Searching for the molecular algorithms of the cell. *Mol. Cell* 49, 202–12.
- (7) Sekine, R., Yamamura, M., Ayukawa, S., Ishimatsu, K., Akama, S., Takinoue, M., Hagiya, M., and Kiga, D. (2011) Tunable synthetic phenotypic diversification on Waddington's landscape through autonomous signaling. *Proc. Natl. Acad. Sci. U.S.A.* 108, 17969–73.
- (8) Kobayashi, H., Kaern, M., Araki, M., Chung, K., Gardner, T. S., Cantor, C. R., and Collins, J. J. (2004) Programmable cells: Interfacing natural and engineered gene networks. *Proc. Natl. Acad. Sci. U.S.A.* 101, 8414–9.
- (9) Wu, M., Su, R. Q., Li, X., Ellis, T., Lai, Y. C., and Wang, X. (2013) Engineering of regulated stochastic cell fate determination. *Proc. Natl. Acad. Sci. U.S.A.*, DOI: 10.1073/pnas.1305423110.
- (10) Guantes, R., and Poyatos, J. F. (2008) Multistable decision switches for flexible control of epigenetic differentiation. *PLoS Comput. Biol.* 4, e1000235.
- (11) Zhou, J. X., Brusch, L., and Huang, S. (2011) Predicting pancreas cell fate decisions and reprogramming with a hierarchical multi-attractor model. *PLoS One* 6, e14752.
- (12) Macia, J., Widder, S., and Sole, R. (2009) Why are cellular switches Boolean? General conditions for multistable genetic circuits. *J. Theor. Biol.* 261, 126–35.
- (13) Golubitsky, M.; Stewart, I.; Schaeffer, D. (1988) *Singularities and Groups in Bifurcation Theory*, Springer, New York.
- (14) Gillespie, D. (2001) Approximate accelerated stochastic simulation of chemically reacting systems. *J. Chem. Phys.* 115, 1716–1733.
- (15) Rizk, A., Batt, G., Fages, F., and Soliman, S. (2009) A general computational method for robustness analysis with applications to synthetic gene networks. *Bioinformatics* 25, i169–78.
- (16) Kay, R. R. (2002) Chemotaxis and cell differentiation in *Dictyostelium*. *Curr. Opin. Microbiol.* 5, 575–9.
- (17) Thorel, F., Nepote, V., Avril, I., Kohno, K., Desgraz, R., Chera, S., and Herrera, P. L. (2010) Conversion of adult pancreatic alpha-cells to beta-cells after extreme beta-cell loss. *Nature* 464, 1149–54.
- (18) Aguirre, A., Rubio, M. E., and Gallo, V. (2010) Notch and EGFR pathway interaction regulates neural stem cell number and self-renewal. *Nature* 467, 323–7.
- (19) Matsuzaki, J., Tsuji, T., Imazeki, I., Ikeda, H., and Nishimura, T. (2005) Immunosteroid as a regulator for Th1/Th2 balance: Its possible role in autoimmune diseases. *Autoimmunity* 38, 369–75.
- (20) Tsai, S. L., Goyal, G., and Chen, W. (2010) Surface display of a functional minicellulosome by intracellular complementation using a synthetic yeast consortium and its application to cellulose hydrolysis and ethanol production. *Appl. Environ. Microbiol.* 76, 7514–20.